Turbo Detection of Precoded Sphere Packing Modulation Using Four Transmit Antennas for Differential Space-Time Spreading

Mohammed El-Hajjar, *Graduate Student Member, IEEE,* Osamah Alamri, Soon Xin Ng, *Member, IEEE*, and Lajos Hanzo, *Fellow, IEEE*

***Abstract*— This paper presents a novel turbo-detected multi-dimensional Sphere Packing (SP) modulation scheme using four transmit antennas combined with Differentially encoded Space-Time Spreading (DSTS). The DSTS scheme can be readily combined with PSK, QAM as well as SP modulation schemes. The SP-aided DSTS system advocated has low-complexity encoding and decoding algorithms that require no channel knowledge and it is capable of outperforming the DSTS system dispensing with sphere packing. Further system performance improvements can be attained by serially concatenated convolutional encoding combined with a unity-rate code (URC) referred to as a precoder. Then, at the receiver side, iterative decoding is invoked by exchanging extrinsic information between the precoder's decoder as well as the outer Recursive Systematic Convolutional (RSC) code's decoder. Moreover, the convergence behaviour of the proposed system is evaluated with the aid of Extrinsic Information Transfer (EXIT) charts. Explicitly, the turbo-detected precoded DSTS-SP system performs within 1.6 dB of the achievable multiple-input multiple output (MIMO) capacity. Finally, in contrast to an equivalent 0.5 bit/symbol throughput turbo-detected DSTS-SP scheme using no precoding, the turbo-detected precoded DSTS-SP scheme exhibits no error floor.**

***Index Terms*— MIMO, differential space-time spreading, sphere packing modulation, recursive systematic convolutional code, unity rate precoder.**

I. Introduction

THE fundamental limitation of reliable wireless transmissions are imposed by time-varying multipath fading, which has to be countered by sophisticated transceiver design [1], [2]. The family of Space-Time Block Codes (STBC) constitutes an effective multiple-input multiple-output (MIMO) scheme that provides good performance in conjunction with a simple decoding scheme over slow fading channels [3], [4]. Inspired by the philosophy of STBC, Hochwald *et al.* [5] proposed the transmit diversity concept known as Space-Time Spreading (STS) for the downlink of Wideband Code Division Multiple Access (WCDMA) [6] that is capable of achieving the highest possible transmit diversity gain. As a further advance, the concept of combining orthogonal transmit diversity designs with the principle of sphere packing modulation [1] was introduced by Su *et al.* in [8], where it was demonstrated that the proposed Sphere Packing (SP) aided STBC system was capable of outperforming the conventional orthogonal design based STBC schemes of [3], [4].

A common feature of all the above-mentioned schemes is that they use coherent detection, which assumes the availability of accurate channel knowledge at the receiver. In practice, the Channel State Information (CSI) of each link between each transmit and each receive antenna pair has to be estimated at the receiver either blindly or using training symbols. However, channel estimation invoked for all the antennas substantially increases both the cost and complexity of the receiver. Furthermore, when the CSI fluctuates dramatically from burst to burst, an increased number of training symbols has to be transmitted, potentially resulting in an undesirably high transmission overhead and wastage of transmission power. Therefore, it is beneficial to develop low-complexity techniques that do not require any channel information and thus are capable of mitigating the complexity of MIMO-channel estimation. Differential Space-Time Block Codes (DSTBC) were designed by Tarokh *et al.* for two transmit antennas and then they were extended to a higher number of transmit antennas [9], [10]. Motivated by these advances, the authors of [11], [12] developed a DSTBC scheme that supports non-constant modulus constellations combined with both two and four transmit antennas. However, the system eliminates the complexity of the MIMO channel estimation albeit this is achieved at the expense of a 3 dB SNR performance loss compared to the coherently detected system having perfect channel knowledge.

Iterative decoding of spectrally efficient modulation schemes was considered by several authors [1], [13]. In [14], the employment of the turbo principle was considered for iterative soft demapping in the context of multilevel modulation schemes combined with channel decoding, where a soft symbol-to-bit demapper was used between the multilevel demodulator and the binary channel decoder. The iterative soft demapping principle of [14] was extended to SP-aided STBC schemes in [15], where the sphere packing demapper of [8] was modified in [15] for the sake of accepting the *a priori* information passed to it from the channel decoder as extrinsic information. In [16], rate-1 inner codes were employed for de-

Manuscript received September 13, 2006; accepted November 9, 2006. The associate editor coordinating the review of this paper and approving it for publication was A. Svensson. The financial support of Vodafone under the auspices of the Dorothy Hodgkin Postgraduate Award, the Ministry of Higher Education of Saudi Arabia, as well as that of the European Union under the auspices of the Pheonix and Newcom projects is gratefully acknowledged.

The authors are with the University of Southampton (e-mail: lh@ecs.soton.ac.uk).

Digital Object Identifier 10.1109/TWC.2008.060708.

[1] Sphere Packing modulation is different from Sphere Decoding [7].

signing low complexity turbo codes suitable for bandwidth and power limited systems having stringent bit-error-rate (BER) requirements. Recently, studying the convergence behaviour of iterative decoding has attracted considerable attention. In [17], ten Brink proposed the employment of the so-called extrinsic information transfer (EXIT) characteristics between a concatenated decoder's output and input for describing the flow of extrinsic information through the soft-in soft-out constituent decoders.

It was shown in [18] that a potentially high capacity is available, when communicating over MIMO channels using multi-dimensional signal sets. In this contribution, we propose a multi-dimensional space-time coding scheme for exploiting this high capacity potential.

The novelty and rationale of the proposed system can be summarised as follows:

1) *Differential Space-Time Spreading (DSTS) using four transmit antennas is advocated for the sake of achieving a high transmit diversity gain. This facilitates low-complexity differential detection, rather than using a more complex receiver employing both channel estimation and coherent detection. Moreover, the system benefits from the multi-user support capability of the STS scheme. Furthermore, the fourth-order diversity of the system results in a Gaussian-like channel error distribution, which improves the attainable performance of both the channel codec and the additionally used SP modulation scheme.*
2) *Both space-time coding [3], [4] and space-time spreading [5] schemes are suboptimum in the sense that the signals received during the different time slots are detected and designed independently. However, we are actually interested in the joint design of several time-slots' signal, because what matters is the minimisation of the DSTS symbol error probability, rather than that of the symbol error probability of each time slot. This justifies the employment of SP modulation, which maximises the Euclidean distance of the SP symbols, each of which conveys several time-slots' signal.*
3) *The capacity of the noncoherently detected four-dimensional SP-aided system is quantified for transmission over both Rayleigh as well as Gaussian channels. Furthermore, we propose a novel scheme for quantifying the maximum achievable rate of the system using EXIT charts.*
4) *The optimum bit-to-SP-symbol mapper is designed using an EXIT-chart based procedure, which allows us to achieve diverse design objectives. For example, we can design a system having the lowest possible turbo-cliff-SNR, but tolerating the formation of an error floor. Alternatively, we can design a system having no error floor, but having a slightly higher turbo-cliff-SNR.*
5) *Finally, a unity-rate precoder is introduced, which is capable of completely eliminating the system's error-floor as well as operating at the lowest possible turbo-cliff SNR without significantly increasing the associated complexity or interleaver delay.*

Therefore, the paper presents a beneficial amalgam, rather than concatenated conglomerate of the components, designed for eliminating the system's error-floor, while operating at the lowest possible turbo-cliff SNR.

This paper is organised as follows. In Section II, a brief system overview is presented. In Section III, the encoding and decoding algorithms designed for DSTS schemes employing four transmit antennas are described. In Section IV, we demonstrate how the proposed DSTS scheme is designed using SP signal constellations. Section V demonstrates how the DSTS-SP demapper is modified for the sake of exploiting the $a\ priori$ knowledge provided by the channel decoder, while our EXIT chart analysis is provided in Section VI. Capacity analysis is done in Section VII followed by the results in Section VIII. Finally, we conclude in Section IX.

II. System Overview

The schematic of the proposed system is shown in Figure 1, where the transmitted source bits are convolutionally encoded and then interleaved by a random bit interleaver. A $1/2$-rate Recursive Systematic Convolutional (RSC) code was employed. After channel interleaving the symbols are precoded by a unity-rate code (URC) encoder. Then, the SP mapper of Figure 1 maps B_{sp} channel-coded bits $\mathbf{b} = b_{0,\ldots,B_{sp}-1} \in \{0,1\}$ to a sphere packing symbol $\mathbf{s}^l$, $l = 0, 1, \ldots, L-1$, so that we have $\mathbf{s}^l = map_{sp}(\mathbf{b})$, where $B_{sp} = \log_2 L$ and L represents the number of modulated symbols in the sphere-packed signalling alphabet. Subsequently, each of the four components of a four-dimensional SP symbol is transmitted using DSTS via four transmit antennas, as will be detailed in Section IV.

In this contribution, we consider transmissions over a temporally correlated narrowband Rayleigh fading channel, where the channel coefficients are spatially independent, associated with a normalised Doppler frequency of $f_D = f_d T_s = 0.01$, with f_d being the Doppler frequency and T_s the symbol duration. The complex Additive White Gaussian Noise (AWGN) of $n = n_I + jn_Q$ contaminates the received signal, where n_I and n_Q are two independent zero-mean Gaussian random variables having a variance of $N_0/2$ per dimension, with $N_0/2$ representing the double-sided noise power spectral density expressed in W/Hz.

As shown in Figure 1, the received complex-valued symbols are first decoded by the DSTS decoder in order to produce a received SP symbol $\tilde{\mathbf{s}}$, which is fed into the SP demapper. As seen in Figure 1, the URC decoder processes the information forwarded by the SP demapper in conjunction with the $a\ priori$ information in order to generate the $a\ posteriori$ probability. The $a\ priori$ Log-Likelihood Ratio (LLR) values of the URC decoder are subtracted from the $a\ posteriori$ LLR values, provided by the Log Maximum Aposteriori Probability (MAP) algorithm, for the sake of generating the extrinsic LLR values $L_{M,e}$, as seen in Figure 1. Next, the soft bits $L_{D,a}$ are passed to the convolutional decoder of Figure 1 in order to compute the $a\ posteriori$ LLR values $L_{D,p}$ provided by the Log MAP algorithm [19] for all the channel-coded bits. During the last iteration, only the LLR values $L_{D,i,p}$ of the original uncoded systematic information bits are required, which are passed to the hard decision decoder of Figure 1 in order to determine the estimated transmitted source bits. As

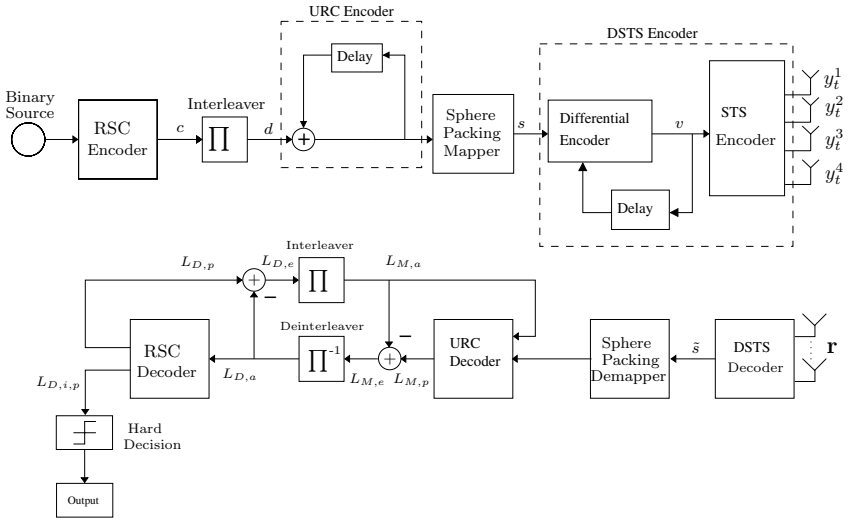

Fig. 1. The Turbo Detection Aided DSTS-SP System.

seen in Figure 1, the extrinsic information $L_{D,e}$, is generated by subtracting the $a\ priori$ information from the $a\ posteriori$ information according to $(L_{D,p} - L_{D,a})$, which is then fed back to the URC decoder as the $a\ priori$ information $L_{M,a}$ after appropriately reordering them using the interleaver of Figure 1. The URC employed is optimal in the sense that it is a memory-1 precoder and thus has the lowest possible decoding complexity. On the other hand, due to the recursive rate-1 precoder, the EXIT curves converge to the $(1.0, 1.0)$ point as shown in Figure 3. Therefore, the precoder employed increases the efficiency of information exchange with the outer SISO channel decoder.

The structure of the binary benchmarker scheme is identical to the scheme seen in Figure 1, except that the URC inner code is not employed and hence iterative decoding is carried out between the outer convolutional code and the inner sphere packing demapper.

III. DSTS Design Using Four Transmit Antennas and Real-Valued Constellations

As widely recognised, coherent detection schemes require CSI, which is acquired by transmitting training symbols. However, high-accuracy multi-antenna channel estimation imposes a high complexity on the receiver. This renders differential encoding and decoding an attractive design alternative, despite the associated E_b/N_0 loss.

The transmitted and received DSTS symbols are encoded and decoded based on the differential relationship among subsequent symbols, as illustrated for classic QAM in [2, Chapter 11]. For the sake of simplicity, we consider having a single receive antenna, although the extension to systems having more than one receive antenna is straightforward.

According to Figure 1, it becomes clear that the DSTS encoder can be divided into two main stages. The differential encoding takes place before space-time spreading and the differentially encoded symbols are then spread as illustrated in [5], [6], where 4 bits are transmitted using four transmit antennas within four time slots.

The DSTS encoding/decoding algorithms operate as follows. At time instant $t = 0$, the arbitrary dummy reference symbols v_0^1, v_0^2, v_0^3 and v_0^4 are transmitted from antennas one, two, three and four, respectively. At time instants $t \geq 1$, a block of $4B$ bits arrives at the bits-to-symbols mapper, where each set of B bits is mapped to a real-valued modulated symbol a_t^k, $k = 1, 2, 3, 4$, selected from a 2^B-ary constellation. Note that B_{sp} mentioned in Section II is equal to $4B$ and was used to differentiate between the number of bits required for SP and that for conventional schemes as will be detailed in Section IV. Assume that v_t^k, $k = 1, 2, 3, 4$, are the differentially encoded symbols. Then, differential encoding is carried out as follows:

$$\mathbf{V_t} = \begin{pmatrix} v_t^1 \\ v_t^2 \\ v_t^3 \\ v_t^4 \end{pmatrix} = a_t^1 \cdot \begin{pmatrix} v_{t-1}^1 \\ v_{t-1}^2 \\ v_{t-1}^3 \\ v_{t-1}^4 \end{pmatrix} + a_t^2 \cdot \begin{pmatrix} v_{t-1}^2 \\ -v_{t-1}^1 \\ v_{t-1}^4 \\ -v_{t-1}^3 \end{pmatrix} + a_t^3 \cdot \begin{pmatrix} v_{t-1}^3 \\ -v_{t-1}^4 \\ -v_{t-1}^1 \\ v_{t-1}^2 \end{pmatrix} + a_t^4 \cdot \begin{pmatrix} v_{t-1}^4 \\ v_{t-1}^3 \\ -v_{t-1}^2 \\ -v_{t-1}^1 \end{pmatrix}. \quad (1)$$

The vector $\mathbf{V_t}$ of Equation (1) is normalised by the magnitude of the previously computed vector $\mathbf{V_{t-1}}$ before transmission in order to limit the peak power and hence the out-of-band power emissions.

The differentially encoded symbols are then spread with the aid of the spreading codes $\mathbf{c_1}$, $\mathbf{c_2}$, $\mathbf{c_3}$, and $\mathbf{c_4}$, which are generated from the same user-specific spreading code $\mathbf{c}$ by ensuring that they are orthogonal using the simple code-concatenation rule of Walsh-Hadamard codes, yielding longer codes and hence a proportionately reduced per antenna throughput according to: $\mathbf{c_1^T} = [\mathbf{c} \quad \mathbf{c} \quad \mathbf{c} \quad \mathbf{c}]$, $\mathbf{c_2^T} = [\mathbf{c} \quad -\mathbf{c} \quad \mathbf{c} \quad -\mathbf{c}]$, $\mathbf{c_3^T} = [\mathbf{c} \quad \mathbf{c} \quad -\mathbf{c} \quad -\mathbf{c}]$, and $\mathbf{c_4^T} = [\mathbf{c} \quad -\mathbf{c} \quad -\mathbf{c} \quad \mathbf{c}]$, where the superscript $^{\mathbf{T}}$ denotes the transpose of the vector.

The differentially encoded data is then divided into four quarter-rate substreams and the four consecutive symbols are then spread to the four transmit antennas according to the

following derived equations:

$$\mathbf{y}_t^1 = \frac{1}{\sqrt{4}}\left(\mathbf{c_1}\cdot v_t^1 - \mathbf{c_2}\cdot v_t^2 - \mathbf{c_3}\cdot v_t^3 - \mathbf{c_4}\cdot v_t^4\right) \quad (2)$$

$$\mathbf{y}_t^2 = \frac{1}{\sqrt{4}}\left(\mathbf{c_1}\cdot v_t^2 + \mathbf{c_2}\cdot v_t^1 + \mathbf{c_3}\cdot v_t^4 - \mathbf{c_4}\cdot v_t^3\right) \quad (3)$$

$$\mathbf{y}_t^3 = \frac{1}{\sqrt{4}}\left(\mathbf{c_1}\cdot v_t^3 - \mathbf{c_2}\cdot v_t^4 + \mathbf{c_3}\cdot v_t^1 + \mathbf{c_4}\cdot v_t^2\right) \quad (4)$$

$$\mathbf{y}_t^4 = \frac{1}{\sqrt{4}}\left(\mathbf{c_1}\cdot v_t^4 + \mathbf{c_2}\cdot v_t^3 - \mathbf{c_3}\cdot v_t^2 + \mathbf{c_4}\cdot v_t^1\right). \quad (5)$$

The received signal at the output of the single receiver antenna can be represented as:

$$\mathbf{r}_t = h_1\cdot\mathbf{y}_t^1 + h_2\cdot\mathbf{y}_t^2 + h_3\cdot\mathbf{y}_t^3 + h_4\cdot\mathbf{y}_t^4 + \mathbf{n}_t, \quad (6)$$

where h_1, h_2, h_3, and h_4 denote the narrow-band complex-valued Channel Impulse Responses (CIR) corresponding to the four transmit antennas, where it is assumed that the channel coefficients remain unchanged for two consecutive transmitted vectors $\mathbf{y}^k$, while $\mathbf{n}_t$ is a complex-valued Gaussian random variable having a covariance matrix of $\sigma_n^2\cdot\mathbf{I}_{SF}$, where SF is the spreading factor of the codes $\mathbf{c}_k$, $k=1,2,3,4$, and $\mathbf{I}_{SF}$ is the Identity matrix.

The received signal $\mathbf{r}_t$ is then correlated with $\mathbf{c}_1$, $\mathbf{c}_2$, $\mathbf{c}_3$, and $\mathbf{c}_4$ according to the following operation: $d_t^k = \mathbf{c}_k^\dagger\cdot\mathbf{r}_t$, with $k=1,2,3,4$ and $\dagger$ representing the Hermitian of the vector. After the correlation operation we arrive at four data symbols represented by:

$$d_t^1 = \frac{1}{\sqrt{4}}\left(h_1\cdot v_t^1 + h_2\cdot v_t^2 + h_3\cdot v_t^3 + h_4\cdot v_t^4\right) + \mathbf{c}_1^\dagger\cdot\mathbf{n}_t \quad (7)$$

$$d_t^2 = \frac{1}{\sqrt{4}}\left(-h_1\cdot v_t^2 + h_2\cdot v_t^1 - h_3\cdot v_t^4 + h_4\cdot v_t^3\right) + \mathbf{c}_2^\dagger\cdot\mathbf{n}_t \quad (8)$$

$$d_t^3 = \frac{1}{\sqrt{4}}\left(-h_1\cdot v_t^3 + h_2\cdot v_t^4 + h_3\cdot v_t^1 - h_4\cdot v_t^2\right) + \mathbf{c}_3^\dagger\cdot\mathbf{n}_t \quad (9)$$

$$d_t^4 = \frac{1}{\sqrt{4}}\left(-h_1\cdot v_t^4 - h_2\cdot v_t^3 + h_3\cdot v_t^2 + h_4\cdot v_t^1\right) + \mathbf{c}_4^\dagger\cdot\mathbf{n}_t \quad (10)$$

.

To derive the decoder equations of the DSTS receiver, the received signals in Equations (7)-(10) are rearranged in vectorial form as follows:

$$\mathbf{R}_t^1 = \left(d_t^1, d_t^2, d_t^3, d_t^4\right) \quad (11)$$

$$\mathbf{R}_t^2 = \left(-d_t^2, d_t^1, d_t^4, -d_t^3\right) \quad (12)$$

$$\mathbf{R}_t^3 = \left(-d_t^3, -d_t^4, d_t^1, d_t^2\right) \quad (13)$$

$$\mathbf{R}_t^4 = \left(-d_t^4, d_t^3, -d_t^2, d_t^1\right) \quad (14)$$

$$\mathbf{R}_{t+1} = \left(d_{t+1}^1, d_{t+1}^2, d_{t+1}^3, d_{t+1}^4\right). \quad (15)$$

To decode the transmitted symbols a_t^k, $k=1,2,3,4$, the decoder uses Equations (11)-(15) and computes:

$$Re\{\mathbf{R}_{t+1}\cdot\mathbf{R}_t^{k\dagger}\} = \sum_{i=1}^{4}|h_i|^2\cdot\sqrt{\sum_{j=1}^{4}|v_t^j|^2}\cdot a_{t+1}^k + N_k, \quad (16)$$

where $Re\{\cdot\}$ denotes the $real$ part of a complex number and N_k denotes the noise term having a variance of $2\cdot\sum_{i=1}^{4}|h_i|^2\cdot\sqrt{\sum_{j=1}^{4}|v_t^j|^2}\cdot\sigma_n^2$. The receiver estimates a_t^k based on Equation (16) by employing a Maximum Likelihood (ML) decoder.

IV. DSTS Design Using Sphere Packing Modulation

It was shown in [8] that the so-called diversity product quantifying the achievable coding advantage[2] of an orthogonal transmit diversity scheme is determined by the minimum Euclidean distance of the transmitted signal vectors. Hence, in order to maximise the achievable coding advantage, it was proposed in [8] to use sphere packing schemes that maximise the minimum Euclidean distance of the transmitted signal vectors.

According to Equation (16), the decoded signals represent scaled versions of a_t^1, a_t^2, a_t^3, and a_t^4 corrupted by the complex-valued AWGN. This observation implies that the diversity product of DSTS systems is determined by the minimum Euclidean distance of all legitimate vectors (a_t^1, a_t^2, a_t^3, a_t^4). Our idea is to jointly design the legitimate 4-component vectors (a_t^1, a_t^2, a_t^3, a_t^4) so that they are represented by a single phasor point selected from a sphere packing constellation corresponding to a 4-dimensional real-valued lattice having the best known minimum Euclidean distance in the 4-dimensional real-valued space $\mathbb{R}^4$. For the sake of generalising our treatment, let us assume that there are L legitimate vectors ($a_t^{l,1}$, $a_t^{l,2}$, $a_t^{l,3}$, $a_t^{l,4}$), $l=0,1,\ldots,L-1$, where L represents the number of 4-component sphere-packed modulated symbols. The transmitter, then, has to choose the modulated signal from these L legitimate symbols, where the four elements $a^{l,1}, a^{l,2}, a^{l,3}, a^{l,4}$ are differentially space-time spread and transmitted from the four transmit antennas. The throughput of the system is $(\log_2 L)/T$ bits per channel use, where $T=4$ is the number of time slots required to transmit the four-dimensional SP signal.

In the four-dimensional real-valued Euclidean space $\mathbb{R}^4$, the lattice D_4 is defined as a sphere packing constellation having the best minimum Euclidean distance from all other $(L-1)$ legitimate 4-component constellation points in $\mathbb{R}^4$ [20]. More specifically, D_4 may be defined as a lattice that consists of all legitimate sphere-packed constellation points having integer coordinates $[a^{l,1}\ a^{l,2}\ a^{l,3}\ a^{l,4}]$ subjected to the sphere packing constraint of $a^{l,1}+a^{l,2}+a^{l,3}+a^{l,4}=k$, where k is an even integer [20]. Assuming that $\mathbf{S} = \{\mathbf{s}^l = [a^{l,1}, a^{l,2}, a^{l,3}, a^{l,4}] \in \mathbb{R}^4 : 0 \le l \le L-1\}$ constitutes a set of L legitimate constellation points from the lattice D_4 having a total energy of $E \triangleq \sum_{l=0}^{L-1}(|a^{l,1}|^2 + |a^{l,2}|^2 + |a^{l,3}|^2 + |a^{l,4}|^2)$, and upon introducing the notation

$$\mathbf{C}_l = \sqrt{\frac{2L}{E}}(a^{l,1}, a^{l,2}, a^{l,3}, a^{l,4}), \quad l=0,1,\ldots,L-1, \quad (17)$$

we have a set of constellation symbols, $\{\mathbf{C}_l\colon 0 \le l \le L-1\}$, leading to the design of DSTS signals, whose diversity product

[2]The diversity product or coding advantage was defined as the estimated gain over an uncoded system having the same diversity order as the coded system [8].

is determined by the minimum Euclidean distance of the set of L legitimate constellation points in $\mathbf{S}$.

A *novel* technique introduced in this paper is the mapping of the four-dimensional SP symbols to the four transmit antenna aided DSTS system. The design of SP constellations in this case is different from that in [15], [21], where twin-antenna-based systems were used. In [15], [21] the four components of the 4-dimensional SP symbol were combined according to $\mathbf{C}_l = \sqrt{\frac{2L}{E}}(x^{l,1}, x^{l,2}), l = 0, 1, \ldots, L-1$, with $\{x^{l,1}, x^{l,2}\} = \{a^{l,1} + ja^{l,2}, a^{l,3} + ja^{l,4}\}$ and $\{x^{l,1}, x^{l,2}\}$ are the symbols passed to the differential encoder. However, when using four transmit antennas, every component of the four dimensions is mapped to a different transmit antenna for transmission. Furthermore, a comparison between the two- and four-antenna aided systems has been carried out and the four-antenna aided system resulted in a better performance owing to its higher diversity gain.

V. Soft-In Soft-Out Demapping for Sphere Packing Constellations

Again, for the sake of simplicity, a system having a single receive antenna is considered, although its extension to several receive antennas is feasible. As already discussed in Section III, the detected DSTS signals can be represented by Equation (16), where a received sphere-packed symbol $\tilde{\mathbf{s}}$ is then constructed from the estimates $\tilde{a}^1$, $\tilde{a}^2$, $\tilde{a}^3$ and $\tilde{a}^4$. The received sphere-packed symbol $\tilde{\mathbf{s}}$ can be written as

$$\tilde{\mathbf{s}} = h \cdot \mathbf{s}^l + \mathbf{N}, \tag{18}$$

where we have $h = \sum_{i=1}^{4} |h_i|^2 \cdot \sqrt{\sum_{j=1}^{4} |v_{t-1}^j|^2}$, $\mathbf{s}^l \in \mathbf{S}$, $0 \leq l \leq L-1$, and $\mathbf{N}$ is a four-dimensional Gaussian random variable having a covariance matrix of $\sigma_N^2 \cdot \mathbf{I}_4$, since the SP symbol constellation $\mathbf{S}$ is four-dimensional.

The SP symbol $\tilde{\mathbf{s}}$ carries B_{sp} channel-coded bits $\mathbf{b} = b_{0,\ldots,B_{sp}-1} \in \{0, 1\}$. As discussed in [15], the LLR value of bit k for $k = 0, \ldots, B_{sp} - 1$ can be written as [14], [15] as shown in Equation (19), where $\alpha = h \cdot \sqrt{\frac{2L}{E}}$, $\mathbf{S}_1^k$ and $\mathbf{S}_0^k$ are the subsets of the symbol constellation $\mathbf{S}$, given that we have $\mathbf{S}_1^k \triangleq \{\mathbf{s}^l \in \mathbf{S} : b_k = 1\}$ and likewise, $\mathbf{S}_0^k \triangleq \{\mathbf{s}^l \in \mathbf{S} : b_k = 0\}$. In other words, $\mathbf{S}_i^k$ represents all symbols of the set $\mathbf{S}$, where we have $b_k = i \in \{0, 1\}$, $k = 0, \ldots, B_{sp} - 1$.

Furthermore, when there is no $a\ priori$ information for the SP demapper, the LLR value of bit k for $k = 0, \ldots, B_{sp} - 1$ can be simplified to

$$L(b_k/\tilde{\mathbf{s}}) = \ln \frac{\sum_{\mathbf{s}^l \in S_1^k} \exp\left[-\frac{1}{2\sigma_w^2} (\tilde{\mathbf{s}} - \alpha \cdot \mathbf{s}^l)(\tilde{\mathbf{s}} - \alpha \cdot \mathbf{s}^l)^T \right]}{\sum_{\mathbf{s}^l \in S_0^k} \exp\left[-\frac{1}{2\sigma_w^2} (\tilde{\mathbf{s}} - \alpha \cdot \mathbf{s}^l)(\tilde{\mathbf{s}} - \alpha \cdot \mathbf{s}^l)^T \right]}. \tag{20}$$

VI. EXIT Chart Analysis

The concept of EXIT charts was proposed in [17], [22] for predicting the convergence behaviour of iterative decoders, where the evolution of the input/output mutual information exchange between the inner and outer decoders in consecutive iterations was examined. The application of EXIT charts is based on two main assumptions, which are realistic when using high interleaver lengths, namely that the $a\ priori$ LLR values are fairly uncorrelated and that the Probability Density Function (PDF) of the $a\ priori$ LLR values is Gaussian distributed.

As seen in Figure 1, the inputs of the URC decoder are the noise-contaminated output of the SP demapper and the $a\ priori$ information $L_{M,a}$ generated by the outer channel decoder. The $a\ priori$ information $L_{M,a}$ is subtracted from the URC decoder output $L_{M,p}$ to produce the extrinsic information $L_{M,e}$. Based on the above-mentioned two assumptions, the $a\ priori$ input $L_{M,a}$ can be modelled by applying an independent zero-mean Gaussian random variable n_A having a variance of σ_A^2.

In conjunction with the outer channel coded and interleaved bits $d \in \{0, 1\}$ of Figure 1 or equivalently $x = \mu(d) \in \{-1, +1\}$, where the function $\mu()$ represents the mapping of the interleaved bit d to the symbol x, the $a\ priori$ input $L_{M,a}$ can be written as [17] $L_{M,a} = \mu_A \cdot x + n_A$, where $\mu_A = \sigma_A^2/2$, since $L_{M,a}$ is an LLR-value obeying the Gaussian distribution [23]. Accordingly, the mutual information of $I_{A_M} = I(d; L_{M,a})$, $0 \leq I_{A_M} \leq 1$, between the outer encoded and interleaved bits d as well as the LLR values $L_{M,a}$ is used to quantify the information content of the $a\ priori$ knowledge at the input of the inner decoder [24].

Moreover, the mutual information $I_{E_M} = I(d, L_{M,e})$ can be used to quantify the extrinsic information $L_{M,e}$ at the output of the inner encoder of Figure 1. Finally, I_{E_M} is a function of both I_{A_M} and the E_b/N_0 value encountered.

The extrinsic transfer characteristic of the outer channel decoder describes the relationship between the outer channel coded input $L_{D,a}$ and the outer channel decoded extrinsic output $L_{D,e}$. The input of the outer channel decoder is constituted by the $a\ priori$ input $L_{D,a}$ provided by the URC decoder. Therefore, the extrinsic information transfer characteristics of the outer channel decoder is independent of the E_b/N_0-value and hence may be written as $I_{E_D} = T_D(I_{A_D})$, where $I_{A_D} = I(c; L_{D,a})$, $0 \leq I_{A_D} \leq 1$, is the mutual information between the outer channel coded bits c and the LLR values $L_{D,a}$. Similarly, $I_{E_D} = I(c; L_{D,e})$, $0 \leq I_{E_D} \leq 1$, is the mutual information between the outer channel coded bits c and the LLR values $L_{D,e}$.

The exchange of extrinsic information in the system schematic of Figure 1 is visualised by plotting the EXIT characteristics of the inner URC decoder and the outer RSC decoder in an EXIT chart [17], [22]. The outer RSC decoder's extrinsic output I_{E_D} becomes the URC decoder's $a\ priori$ input I_{A_M}, which is represented on the x-axis. Similarly, on the y-axis, the URC decoder's extrinsic output I_{E_M} becomes the outer RSC decoder's $a\ priori$ input I_{A_D}.

VII. Capacity of the DSTS-SP System

The following capacity analysis has been carried out for the proposed four-antenna aided *differentially encoded* STS-SP system employing a single receive antenna.

For a four-antenna aided transmitter using a single coherent detector provided with perfect knowledge of the channel

$$L(b_k/\tilde{\mathbf{s}}) = L_a(b_k) + \ln \frac{\sum_{\mathbf{s}^l \in S_1^k} \exp\left[-\frac{1}{2\sigma_w^2}(\tilde{\mathbf{s}} - \alpha \cdot \mathbf{s}^l)(\tilde{\mathbf{s}} - \alpha \cdot \mathbf{s}^l)^T + \sum_{j=0, j\neq k}^{B-1} b_j L_a(b_j) \right]}{\sum_{\mathbf{s}^l \in S_0^k} \exp\left[-\frac{1}{2\sigma_w^2}(\tilde{\mathbf{s}} - \alpha \cdot \mathbf{s}^l)(\tilde{\mathbf{s}} - \alpha \cdot \mathbf{s}^l)^T + \sum_{j=0, j\neq k}^{B-1} b_j L_a(b_j) \right]}$$
$$= L_{M,a} + L_{M,e}. \tag{19}$$

coefficients at the receiver, the Continuous-Input Continuous-Output Memoryless Channel's (CCMC) [25] bandwidth efficiency can be formulated as follows [26]:

$$\eta_{coherent}^{CCMC}(SNR) = E\left[\log_2\left(1 + \sum_{i=1}^{4} |h_i|^2 \frac{SNR}{4}\right)\right] \text{ [b/s/Hz]}, \tag{21}$$

where the expectation $E[.]$ is taken over $\sum_{i=1}^{4} |h_i|^2$ and h_i represents the CIR between transmit antenna i and the receive antenna.

Furthermore, the CCMC's bandwidth efficiency for a single-transmit single-receive antenna non-coherent system was given in [27] for high SNR values as follows:

$$\eta_{noncoherent}^{CCMC}(SNR) \approx \frac{T-1}{T}\eta_{coherent}^{CCMC}(SNR) + \frac{1}{T}\log_2\left[\left(\frac{T}{e}\right)^{T-1}\frac{1}{(T-1)!}\right] \text{ [b/s/Hz]}, \tag{22}$$

where T is the coherence time of the system.

It was argued in [18] that a STBC-aided MIMO system can be transformed into a single-input multiple-output (SIMO) system. Using the same reasoning, our DSTS-aided four-antenna system can be transformed into a single transmit antenna system, where the equivalent Rayleigh fading coefficient between the transmitter and the receiver is given by $h = \sum_{i=1}^{4} |h_i|^2 \times \sqrt{\sum_{j=1}^{4} |v_t^j|^2}$ and the equivalent noise at the receiver is given by $\mathbf{N}$ according to Equation (18). More explicitly, according to Equation (18), the received sphere packed signal can be represented as:

$$\tilde{\mathbf{s}} = \sum_{i=1}^{4} |h_i|^2 \cdot \sqrt{\sum_{j=1}^{4} |v_t^j|^2} \cdot \mathbf{s}^l + \mathbf{N} = h \cdot \mathbf{s}^l + \mathbf{N}, \tag{23}$$

where we define $\tilde{\mathbf{s}} = (\tilde{a}^1, \tilde{a}^2, \tilde{a}^3, \tilde{a}^4)$ as the received signal vector, $h = \sum_{i=1}^{4} |h_i|^2 \cdot \sqrt{\sum_{j=1}^{4} |v_t^j|^2}$ represents a chi-squared distributed random variable and $\mathbf{N}$ is a four-dimensional Gaussian random variable having a covariance matrix of $\sigma_N^2 \cdot \mathbf{I}_4$, where $\sigma_N^2 = h \cdot N_0/2$ per dimension. When appropriately normalising the transmitted phasor constellation points, we have $\sqrt{\sum_{j=1}^{4} |v_t^j|^2} = 1$ and $h = \sum_{i=1}^{4} |h_i|^2$.

The conditional probability of receiving a specific 4-dimensional signal vector $\tilde{\mathbf{s}}$ given that the 4-dimensional signal $\mathbf{s}^l$, $l \in \{0, \ldots, L-1\}$ was transmitted, can be shown to be:

$$p(\tilde{\mathbf{s}}|\mathbf{s}^l) = \frac{1}{(\pi N_0 h)^2} \exp\left(\sum_{i=1}^{4} \frac{-\left|\tilde{\mathbf{s}}[i] - h \cdot \mathbf{s}^l[i]\right|^2}{hN_0}\right). \tag{24}$$

The four-dimensional SP constellation used has 16 possible equiprobable symbols transmitted during a four-time-slot interval, with each SP symbol carrying $\log_2(16) = 4$ bits. Therefore, the Discrete-Input Continuous-Output Memoryless Channel's (DCMC) [25] capacity for the 4-dimensional SP modulation assisted four transmit antenna based DSTS scheme can be computed according to [18] as:

$$C_{DSTS-SP}^{DCMC}(SNR) = \log_2(L) - \frac{1}{L}\sum_{m=1}^{L} E\left[\log_2 \sum_{n=1}^{L} exp(\Psi_{m,n}) \;\middle|\; \mathbf{s}^l\right] \text{ [bits/sym]}, \tag{25}$$

where $E[A|\mathbf{s}^l]$ is the expectation of A conditioned on $\mathbf{s}^l$ and we have:

$$\Psi_{m,n} = \sum_{d=1}^{4} \frac{-|h\,(\mathbf{s}^m[d] - \mathbf{s}^n[d]) + \mathbf{N}[d]|^2 + |\mathbf{N}[d]|^2}{hN_0}. \tag{26}$$

The bandwidth efficiency of the DCMC for our four transmit antenna based DSTS-SP system is determined by normalising the channel capacity with respect to the constellation dimension D as follows [18]:

$$\eta_{DSTS-SP}^{DCMC}(SNR) = \frac{C_{DSTS-SP}^{DCMC}(SNR)}{D/2} \quad \text{[b/s/Hz]}. \tag{27}$$

It was argued in [28], [29] that the maximum achievable bandwidth efficiency of the system is equal to the area under the EXIT curve of the inner code provided that the bit stream $\mathbf{b}$ has independently and uniformly distributed bits, the channel is an erasure channel, the inner code rate is 1 and the MAP algorithms is used for decoding. Assuming that the area under the EXIT curve of the inner decoder, i.e. the URC decoder and the SP demapper, is represented by $\mathcal{A}$, the *maximum* attainable rate for the outer code is given by $R_{max} = \mathcal{A}$ [28] at a specific E_b/N_0 value. Therefore, the maximum achievable bandwidth efficiency becomes $\eta_{max} = Q \times R_{max}$, where Q is the number of bits per symbol in the DSTS-SP system.

The MIMO channel capacity curves of the 4-dimensional SP modulation assisted four transmit antenna aided DSTS scheme are shown in Figure 2, portraying both the DCMC and CCMC capacity curves as well as the maximum achievable rate of the system derived from the EXIT curves. Observe that there is a gap between the DCMC capacity and CCMC capacity. The attainable capacity is similar to that of the M-ary orthogonal signalling scheme of [2], where it was shown that the DCMC bandwidth efficiency exhibits an increasingly higher discrepancy with respect to the CCMC bandwidth efficiency, as the number of dimensions is reduced. The reason for this observation is the fact that the proposed four transmit antenna aided system is capable of accommodating 8-dimensions

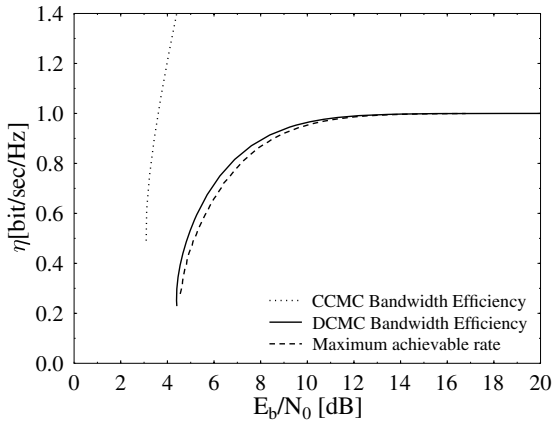

Fig. 2. Capacity of the four transmit antenna aided DSTS-SP system for both Rayleigh and AWGN channels in conjunction with L=16.

by exploiting both the in-phase and quadrature components of each antenna. However, in our system we only used the in-phase component, which exploited only four dimensions out of the eight available dimensions. At a bandwidth efficiency of $\eta = 0.5$ bit/s/Hz, the CCMC and DCMC capacity limits are $E_b/N_0 \approx 3.1$ dB and $E_b/N_0 \approx 4.9$ dB, respectively. Furthermore, observe in Figure 2 that the maximum achievable rate of the system derived from the EXIT curves is quite close to the DCMC capacity. Note that the maximum attainable rate obtained from the EXIT charts would resemble the capacity limit, provided that the MAP algorithm [30] is employed by the constituent decoders. However, our DSTS decoder employs a very simple decoding algorithm that utilises only two consecutively received symbols despite the fact that all the symbols are interdependent. Therefore, the decoder employed is suboptimum and if a trellis based DSTS decoder such as the MAP algorithm [30] is employed, then the maximum achievable rate obtained from the EXIT chart might match the capacity limit computed. Nevertheless, the complexity of the MAP algorithm is high in return for a modest gain of 0.2 dB, as seen in Figure 2.

VIII. Results and Discussion

In this section, we consider a four-transmit-antenna DSTS-SP system associated with $L = 16$ and a single receiver antenna, in order to demonstrate the performance improvements achieved by the proposed system. All simulation parameters are listed in Table I, where RSC(2,1,5) is a half rate RSC code having a constraint length of 5.

It was shown in [20] that there is a total of 24 legitimate symbols[3] hosted by D_4 having an identical minimum energy of $E = 2$. It is desirable to choose a specific subset of $L = 16$ 4-component points from the entire set of legitimate constellation points hosted by D_4, which possesses the highest minimum Euclidean distance, hence minimising the error probability. Therefore, we used a computer search for determining the optimum choice of the $L = 16$ points out of the possible 24 points.

As shown in [14], Gray mapping combined with iterative demapping and decoding does not result in any performance improvements. Therefore, Anti-Gray Mapping (AGM) schemes have been developed, where extrinsic information is exchanged between the channel decoder and the SP symbol-to-bit demapper. Any mapping which is different from the classic Gray mapping may be referred to as AGM. We evaluated the performance of all legitimate AGM schemes in order to find the best performer. In this paper we used two different AGM schemes referred to as AGM-1 and AGM-2, where AGM-1 is considered as the optimum mapping, i.e. the mapping having the highest intersection point between the EXIT curves of the channel decoder and the SP symbol-to-bit demapper. Both the GM and AGM schemes are listed in Table II.

Figure 3 plots the EXIT charts of the turbo-detection aided channel-coded DSTS-SP system employing Gray mapping (GM) in conjunction with the outer $1/2$-rate RSC code, the

[3]In simple terms, the sphere centred at $(0, 0, 0, 0)$ has 24 spheres around it, centred at the points $(+/-1, +/-1, 0, 0)$, where any choice of signs and any ordering of the coordinates is legitimate [20, p.9].

TABLE I
System Parameters

Sphere Packing Modulation	$L = 16$
No. of Transmitter Antennas	4
No. of Receiver Antennas	1
Channel	Correlated Rayleigh Fading
Normalised Doppler frequency	0.01
Outer channel Code Generator	RSC $(2, 1, 5)$ (g_r, g)=$(35, 23)_8$
Precoder Generator	URC $G(D)$=$1/(1 + D)$ D represents a Delay element
Spreading Code	Walsh Code
Spreading Factor	8
Number of users	4

TABLE II
Bit mappings for the Gray Mapping (GM) and the two different anti-Gray mapping schemes AGM-1 and AGM-2 introduced in Section VIII for four transmit antennas DSTS-SP signals of size $L = 16$.

Points from D_4				Integer Index		
a_1	a_2	a_3	a_4	GM	AGM-1	AGM-2
−1	−1	0	0	0	0	15
0	−1	−1	0	1	11	1
0	−1	+1	0	2	7	2
+1	−1	0	0	3	12	3
−1	0	0	+1	4	14	4
0	0	−1	+1	5	5	5
0	0	+1	+1	6	9	6
+1	0	0	+1	7	2	7
−1	0	0	−1	8	13	8
0	0	−1	−1	9	6	9
0	0	+1	−1	10	10	10
+1	0	0	−1	11	1	11
−1	+1	0	0	12	3	12
0	+1	−1	0	13	8	13
0	+1	+1	0	14	4	14
+1	+1	0	0	15	15	0

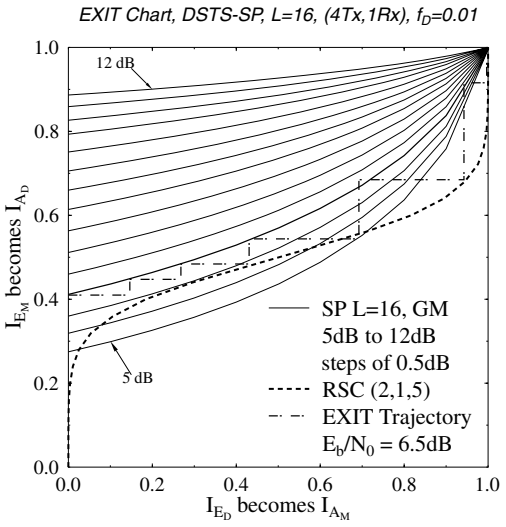

Fig. 3. EXIT chart of a $1/2$-rate RSC channel-coded and precoded DSTS-SP scheme employing Gray mapping aided SP in conjunction with $L = 16$, while using an interleaver length of $D = 1,000,000$ bits, $I = 10$ iterations and the system parameters outlined in Table I.

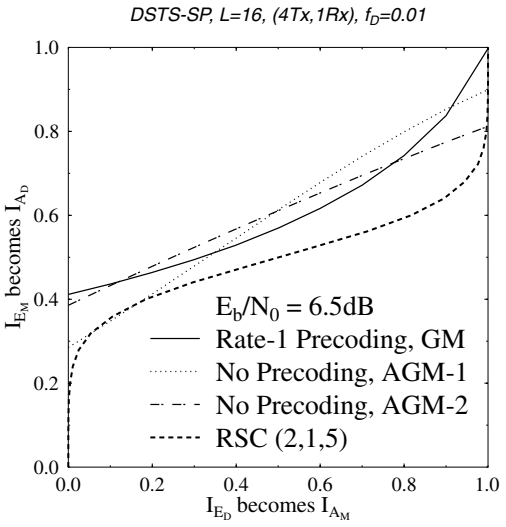

Fig. 4. Comparison of the convergence behaviour of both the precoded and non-precoded system based on the EXIT chart, while using an interleaver length of $D = 1,000,000$ bits, $I = 10$ iterations and the system parameters outlined in Table I, when operating at an E_b/N_0 of 6.5 dB.

inner URC and the system parameters outlined in Table I for different E_b/N_0 values. The GM was used in this case because no iterations are invoked between the SP demapper and the decoders and thus, in this case, it is better to use GM that results in a higher initial mutual information and hence a higher starting point in the EXIT curve. Ideally, in order for the exchange of extrinsic information between the URC's decoder and the RSC decoder to converge at a specific E_b/N_0 value, the EXIT curve of the URC decoder and that of the outer RSC decoder should only intersect at a point near the $I_{E_D} = 1.0$ line. If this condition is satisfied, then a so-called open *convergence tunnel* [17], [22] appears in the EXIT chart. It is plausible that the narrower the tunnel, the more iterations are required for reaching the $I_{E_D} = 1.0$ line. Observe from the figure that an open convergence tunnel is formed around $E_b/N_0 = 6.5$ dB. This implies that according to the predictions of the EXIT chart seen in Figure 3, the iterative decoding process is expected to converge at an E_b/N_0 value between 6.0 dB and 6.5 dB. The EXIT chart based convergence predictions can be verified by the actual iterative decoding trajectory of Figure 3, where the trajectory was recorded at $E_b/N_0 = 6.5$ dB while using an interleaver length of $D = 100,000$ bits. The steps seen in the figure represent the actual extrinsic information exchange between the URC's decoder and the outer RSC channel decoder. Since a long interleaver is employed, the assumptions outlined at the beginning of Section VI are justified and hence the EXIT chart based convergence prediction becomes accurate.

Furthermore, our convergence comparison of the precoded and the non-precoded systems is shown in Figure 4 for E_b/N_0 values of 6.5 dB. Observe in Figure 4 that when no precoding is employed, the AGM-1 scheme has no open convergence tunnel at $E_b/N_0 = 6.5$ dB, while the nonprecoded AGM-2 and the precoded GM-based systems do converge at $E_b/N_0 =$

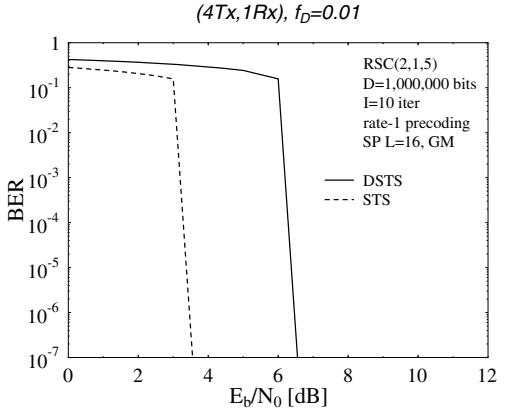

Fig. 5. Performance comparison of the coherently detected and the differentially detected space-time spreading schemes employing SP in conjuction with $L = 16$, while using rate-1 precoding while using an interleaver length of $D = 1,000,000$ bits, $I = 10$ iterations and the system parameters outlined in Table I.

6.5 dB. However, as the E_b/N_0 increases to 7 dB, the nonprecoded AGM-1 scheme exhibits an open convergence tunnel. Furthermore, the AGM-2 scheme of Table II converges at a lower E_b/N_0 value, while the AGM-1 scheme attains a lower BER. This observation is based on the fact that the EXIT curve of the AGM-1 arrangement intersects the EXIT curve of the outer decoder at a higher point than the AGM-2 scheme of Table II. This will be further substantiated in Figure 6. Furthermore, observing the precoded system of Figure 3 employing GM, we note that the intersection point between the EXIT curves of the URC decoder and the outer RSC decoder is at $I_{E_D} = 1.0$, hence we have in an infinitesimally low BER.

A comparison between the coherently detected and the dif-

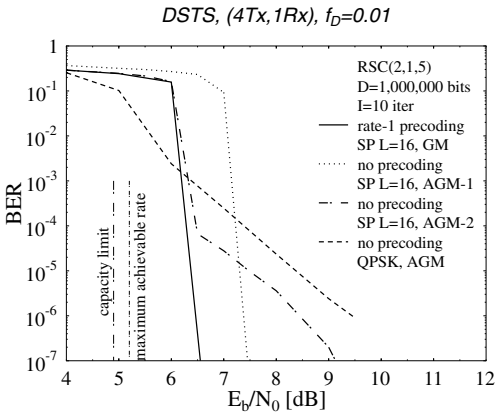

Fig. 6. Performance comparison of AGM-1 and AGM-2 based convolutional-coded DSTS-SP schemes in conjuction with $L = 16$, while using no precoding together with the system employing a precoder and GM, while using an interleaver length of $D = 1,000,000$ bits, $I = 10$ iterations and the system parameters outlined in Table I.

ferentially detected space-time spreading schemes employing SP in conjuction with $L = 16$ in shown in Figure 5. The system employs a rate-1 precoder, while using an interleaver length of $D = 1,000,000$ bits, $I = 10$ iterations and the system parameters outlined in Table I. The coherent system employed in this paper assumes the availability of perfect channel knowledge at the receiver side. As shown in the figure, coherent detection with perfect channel knowledge results in an almost 3 dB E_b/N_0 gain over the differentially encoded and decoded signals. This is simply due to the error-doubling property of differential detection.

Finally, Figure 6 provides a performance comparison between three 0.5 BPS-throughput DSTS schemes, namely those of the precoded system employing GM and non-precoded systems employing AGM-1 and AGM-2, while using $L = 16$ and the best possible Anti-Gray Mapping [31] based $1/2$-rate RSC-coded non-precoded DSTS-QPSK scheme. The system employs an interleaver length of $D = 1,000,000$ bits, $I = 10$ iterations and the system parameters of Table I. Moreover, the figure plots the achievable capacity as well as the maximum achievable rate obtained from the EXIT charts of the four transmit antenna aided DSTS-SP system having a spectral efficiency of 0.5 bits/sec/Hz. The results of Figure 6 demonstrate that the system employing a $1/2$-rate RSC code without the precoder and using AGM-2 has approached the system capacity quite closely. However as the SNR increases we notice in Figure 6 that the BER performance reaches a point, where further BER improvements require a more substantial SNR increase and this is justified by the EXIT chart of Figure 4. Moreover, the system employing a $1/2$-rate RSC code without the precoder and using AGM-1 converges at $E_b/N_0 = 7.0$ dB to a very low BER as compared to the AGM-2 based system. According to the EXIT chart of Figure 4, the AGM-1 scheme BER performance will reach a point where further BER improvements require a more substantial SNR increase. While this is not explicitly shown in Figure 6, the system performance is expected to reach that point at a BER lower than 10^{-7}. Furthermore, Figure 6 demonstrates that the proposed non-precoded turbo-detected DSTS-SP scheme provides a better performance than the equivalent-throughput DSTS scheme dispensing with SP modulation. More explicitly, the DSTS-SP scheme of Figure 6 using $L = 16$ and AGM-1 exhibits an E_b/N_0 gain of around 2 dB at a BER of 10^{-6} over the identical-throughput 0.5 BPS DSTS-QPSK scheme, while the AGM-2 based system attains an E_b/N_0 gain of around 1 dB. Finally, when a precoder is used, the system's performance improves more dramatically when the SNR is increased, as suggested by the EXIT chart of Figure 3. The precoded system performs within 1.6 dB of the system capacity at a BER of 10^{-7}, which is also within 1.4 dB of the maximum achievable performance computed based on EXIT charts. Furthermore, the precoded system exhibits an E_b/N_0 gain of around 2.6 dB at a BER of 10^{-7} over the identical-throughput 0.5 BPS non-precoded DSTS-SP scheme using AGM-2 and a gain around 1 dB at a BER of 10^{-7} over the identical-throughput 0.5 BPS non-precoded DSTS-SP scheme using AGM-1.

IX. Conclusion

In this paper we proposed a novel system that exploits the advantages of both iterative demapping and turbo detection [14], as well as those of the DSTS-SP scheme developed. The proposed DSTS scheme benefits from a substantial diversity gain, while using four transmit antennas without the need for any CSI. The paper also characterises the benefits of precoding when concatenated with the outer channel code, suggesting that an E_b/N_0 gain of at least 1 dB can be obtained at a BER of 10^{-7}. Furthermore, the system capacity was derived and it was demonstrated that the proposed precoded system performs within 1.6 dB from the system capacity. Explicitly, a 1 BPS four-transmit antenna aided system invoking SP modulation in conjunction with $L = 16$ but no RSC-coding requires an E_b/N_0 of 22 dB at a BER of 10^{-7}, while upon incorporating a $1/2$-rate RSC code together with iterative decoding between the RSC decoder and the SP-demapper requires only an E_b/N_0 of 7.5 dB for maintaining a BER of 10^{-7}. Finally, for the same BER value, the precoded system employed throughout this paper requires an E_b/N_0 of around 6.5 dB. Our future research will consider the design of DSTS schemes that can be generalised to operate in conjunction with arbitrary modulation schemes, while using a near-instantaneously adaptive channel-condition-dependent number of transmit antennas.

References

[1] L. Hanzo, T. H. Liew, B. L. Yeap, *Turbo Coding, Turbo Equalisation and Space Time Coding: For Transmission over Fading Channels*. Chichester, UK: John Wiley and Sons Ltd. and IEEE Press, 2002.

[2] L. Hanzo, S. X. Ng, T. Keller, and W. Webb, *Qaudrature Amplitude Modulation: From Basics to Adaptive Trellis-Coded, Turbo Equalised and Space-Time Coded OFDM, CDMA and MC-CDMA Systems, 2nd Edition*. Chichester, UK: John Wiley and Sons Ltd. and IEEE Press, 2004.

[3] S. M. Alamouti, "A simple transmit diversity technique for wireless communications," *IEEE J. Select. Areas Commun.*, vol. 16, no. 8, pp. 1451–1458, 1998.

[4] V. Tarokh, H. Jafarkhani, and A. R. Calderbank, "Space-time block codes from orthogonal designs," *IEEE Trans. Inf. Theory*, vol. 45, no. 5, pp. 1456–1467, 1999.

[5] B. Hochwald, T. L. Marzetta, and C. B. Papadias, "A transmitter diversity scheme for wideband CDMA systems based on space-time spreading," *IEEE J. Select. Areas Commun.*, vol. 19, no. 1, pp. 48–60, 2001.

[6] L. Hanzo, L.-L. Yang, E.-L. Kaun, and K. Yen, *Single and Multi-Carrier DS-CDMA: Multi-user Detection, Space-Time Spreading, Synchronisation, Networking and Standards*. Chichester, UK: John Wiley and Sons Ltd. and IEEE Press, 2003.

[7] U. Fincke and M. Pohst, "Improved method for calculating vector of short length in a lattice, including a complexity analysis," *Math. Comput.*, vol. 44, pp. 463–471, Apr. 1985.

[8] W. Su, Z. Safar, and K. J. R. Liu, "Space-time signal design for time-correlated Rayleigh fading channels," in *Proc. IEEE International Conference on Communications (ICC)*, vol. 5, pp. 3175–3179, 2003.

[9] V. Tarokh, H. Jafarkhani, "A differential detection scheme for transmit diversity," *IEEE J. Select. Areas Commun.*, vol. 18, no. 7, pp. 1169–1174, 2000.

[10] H. Jafarkhani and V. Tarokh, "Multiple transmit antenna differential detection from generalized orthogonal designs," *IEEE Trans. Inf. Theory*, vol. 47, no. 6, pp. 2626–2631, 2001.

[11] C. Hwang, S. H. Nam, J. Chung, and V. Tarokh, "Differential space time block codes using nonconstant modulus constellations," *IEEE Trans. Signal Processing*, vol. 51, no. 11, pp. 2955–2964, 2003.

[12] S. H. Nam, C. Hwang, J. Chung, and V. Tarokh, "Differential space time block codes using QAM for four transmit antennas," in *IEEE International Conference on Communications*, vol. 2, pp. 952–956, 2004.

[13] S. Le Goff, A. Glavieux, and C. Berrou, "Turbo-codes and high spectral efficiency modulation," in *IEEE International Conference on Communications*, New Orleans, LA, pp. 645–649, 1994.

[14] S. ten Brink, J. Speidel, and R. Yan, "Iterative demapping and decoding for multilevel modulation," in *IEEE Global Telecommunications Conference (GLOBCOM)*, vol. 1, Sydney, NSW, pp. 579–584, 1998.

[15] O. Alamri, B. L. Yeap, L. Hanzo, "A turbo detection and sphere packing modulation aided space-time coding scheme," to appear in *IEEE Trans. Veh. Technol.*, Jan. 2007.

[16] D. Divsalar, S. Dolinar, and F. Pollara, "Serial concatenated trellis coded modulation with rate-1 inner code," in *IEEE Global Telecommunications Conference (GLOBECOM)*, vol. 2, San Francisco, CA, pp. 777–782, 2000.

[17] S. ten Brink, "Designing iterative decoding schemes with the extrinsic information transfer chart," *AEÜ International J. Electron. Commun.*, vol. 54, pp. 389–398, Nov. 2000.

[18] S. X. Ng and L. Hanzo, "On the MIMO channel capacity of multi-dimensional signal sets," *IEEE Trans. Veh. Technol.*, vol. 55, no. 2, pp. 528–536, 2006.

[19] P. Robertson, E. Villebrun, and P. Hoeher, "A comparison of optimal and sub-optimal MAP decoding algorithms operating in the log domain," in *Proc. International Conference on Communications*, Seattle, WA, pp. 1009–1013, June 1995.

[20] J. H. Conway and N. J. Sloane, *Sphere Packings, Lattices and Groups*. Springer-Verlag, 1999.

[21] M. El-Hajjar, O. Alamri, and L. Hanzo, "Differential space-time spreading using iteratively detected sphere packing modulation and two transmit antennas," in *Proc. Wireless Communications and Networking Conference (WCNC)*, Las Vegas, Apr. 2006.

[22] S. ten Brink, "Convergence behavior of iteratively decoded parallel concatenated codes," *IEEE Trans. Commun.*, vol. 49, no. 10, pp. 1727–1737, 2001.

[23] J. Hagenauer, E. Offer, and L. Papke, "Iterative decoding of binary block and convolutional codes," *IEEE Trans. Inf. Theory*, vol. 42, no. 2, pp. 429–445, 1996.

[24] T. M. Cover and J. A. Thomas, *Elements of Information Theory*. New York: Wiley, 1991.

[25] J. G. Proakis, *Digital Communications*. McGraw-Hill, 2001.

[26] E. Telatar, "Capacity of multi-antenna Gaussian channels," *European Trans. Telecommun.*, vol. 10, pp. 585–595, Nov./Dec. 1999.

[27] L. Zheng and D. Tse, "Communication on the Grassmann manifold: a geometric approach to the noncoherent multiple-antenna channel," *IEEE Trans. Inf. Theory*, vol. 48, no. 2, pp. 359–383, 2002.

[28] M. Tüchler, "Design of serially concatenated systems depending on the block length," *IEEE Trans. Commun.*, vol. 52, no. 2, pp. 209–218, 2004.

[29] A. Ashikhmin, G. Kramer, and S. ten Brink, "Extrinsic information transfer functions: model and erasure channel properties," *IEEE Trans. Inf. Theory*, vol. 50, no. 11, pp. 2657–2673, 2004.

[30] L. Bahl, J. Cocke, F. Jelinek, and J. Raviv, "Optimal decoding of linear codes for minimizing symbol error rate (corresp.)," *IEEE Trans. Inf. Theory*, vol. 20, no. 2, pp. 284–287, 1974.

[31] G. Ungerboeck, "Channel coding with multilevel/phase signals," *IEEE Trans. Inf. Theory*, vol. 28, no. 1, pp. 55–67, 1982.

Mohammed El-Hajjar received the B.Eng. degree (with Distinction) in Electrical Engineering from the American University of Beirut (AUB), Lebanon, and the M.Sc. degree (with Distinction) in Radio Frequency Communication Systems from the University of Southampton, UK. Since October 2005, he has been working towards his Ph.D. degree with the Communications Group, School of Electronics and Computer Science, University of Southampton, U.K. Mohammed is the recepient of several academic awards from the AUB as well as the University of Southampton. His research interests include sphere packing modulation, space-time coding, differential space-time spreading, adaptive transceiver design and cooperative communications.

Osamah Rashed Alamri received his B.S. degree with first class honours in electrical engineering from King Fahd University of Petroleum and Minerals (KFUPM), Dhahran, Saudi Arabia, in 1997, where he was ranked first with a 4.0 GPA. In 2002, he received his M.S. degree in electrical engineering from Stanford University, California, USA. Mr. Alamri submitted his PhD thesis in October 2006 and published in excess of 20 research papers while working towards his PhD degree with the Communications Group, Shool of Electronics and Computer Science, University of Southampton, UK. His research interests include sphere packing modulation, space-time coding, turbo coding and detection, multi-dimensional mapping and MIMO systems.

Soon Xin Ng (S'99-M'03) received the B.Eng. degree (First class) in electronics engineering and the Ph.D. degree in wireless communications from the University of Southampton, Southampton, U.K., in 1999 and 2002, respectively. From 2003 to 2006, he was a postdoctoral research fellow working on collaborative European research projects known as SCOUT, NEWCOM and PHOENIX. Since August 2006, he has been a lecturer in wireless communications at the University of Southampton. His research interests are mainly in adaptive coded modulation, channel coding, space-time coding, joint source and channel coding, OFDM and MIMO. He has published numerous papers and coauthored a book in this field.

Lajos Hanzo is a Fellow of the Royal Academy of Engineering. He received his first-class degree in electronics in 1976 and his doctorate in 1983. In 2004 he was awarded the Doctor of Sciences (DSc) degree by the University of Southampton, UK. During his career in telecommunications he has held various research and academic posts in Hungary, Germany and the UK. Since 1986 he has been with the Department of Electronics and Computer Science, University of Southampton, UK, where he holds the chair in telecommunications. He has co-authored 15 books, totalling 10 000 pages on mobile radio communications, published in excess of 700 research papers, has acted as TPC Chair of numerous major IEE and IEEE conferences, presented various keynote lectures and has been awarded a number of distinctions. Currently he heads an academic research team, working on a range of research projects in the field of wireless multimedia communications sponsored by industry, the Engineering and Physical Sciences Research Council (EPSRC) UK, the European IST Programme and the Mobile Virtual Centre of Excellence (VCE), UK. He is an enthusiastic supporter of industrial and academic liaison and he offers a range of industrial courses. Lajos is also an IEEE Distinguished Lecturer of both the Communications as well as the Vehicular Technology Society, a Fellow of both the IEEE and the IEE. He is an editorial board member of the *Proceedings of the IEEE* and a Governor of both the IEEE Communications and VT Society. He was appointed as Editor-in-Chief of the IEEE Press for 2008 - 2009. For further information on research in progress and associated publications, please refer to http://www-mobile.ecs.soton.ac.uk.